Two-Photon Microscopic Measurement of Oxygen Distribution in Mouse Cerebral Microvasculature

95.12/WW2

Sava Sakadžić,[1] Emiri T. Mandeville,[2] Anna Devor,[1,3,4] Mohammad A. Yaseen,[1] Joseph J. Musacchia,[1] Louis Gagnon,[1] Emmanuel Roussakis,[5] Katharina Ekermann-Haerter,[6] Vivek J. Srinivasan,[1] Cenk Ayata,[6,7] Eng H. Lo,[5] Anders M. Dale,[3,4] Sergei A. Vinogradov,[5] and David A. Boas[1]

[1]Optics Division, MGH/MIT/HMS Athinoula A. Martinos Center for Biomedical Imaging, Department of Radiology, MGH/HMS, Charlestown, MA; [2]Neuroprotection Research Laboratory, Departments of Radiology and Neurology, MGH/HMS, Charlestown, MA; [3]Departments of Neurosciences, and [4]Radiology, University of California, San Diego, CA; [5]Department of Biochemistry and Biophysics, University of Pennsylvania, Philadelphia, PA; [6]Neurovascular Research Laboratory, Department of Radiology, MGH/HMS, Charlestown, MA; [7]Stroke Service and Neuroscience Intensive Care Unit, Department of Neurology, MGH/HMS, Boston, MA

Summary

We applied novel pO_2 measurement technology based on two-photon-enhanced phosphorescent nanoprobe to obtain extensive pO_2 maps in cortical microvasculature of mice. Measurement through a sealed cranial window reveals steep pO_2 gradients around both pial and descending arterioles. In contrast, pO_2 maps around ascending venules and capillaries indicate significant heterogeneity of the tissue oxygen concentration in venous and capillary compartments. We analyzed O2 context in all segments of the microvasculature based on branching order from the pial vessels and confirmed significant delivery of oxygen from the precapillary vessels during resting state. In comparison to the resting state, respiration from the capillaries was significantly increased during hypecapnia.

Methods

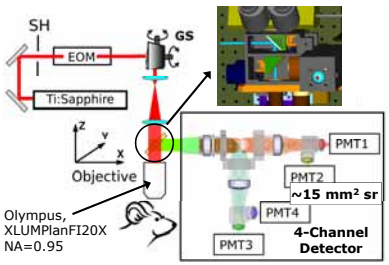

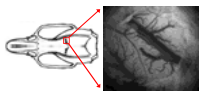

Imaging was performed using custom-built 2-photon microscope through a sealed cranial window over SI area. Mice were anesthetized with isoflurane. BP, HR, expired CO_2 and temperature were monitored. Phosphorescent dye PtP-C343 was dissolved in saline and injected IV.

O_2-Sensitive 2-Photon Enhanced Porphyrin-Based Dye PtP-C343

- O_2 – dependent phosphorescence quenching: pO_2 → lifetime ↓
- λ_{ex} = 840 nm, λ_{em} = 690 nm
- $pO_2 = \left(\frac{1}{\tau} - \frac{1}{\tau_0}\right)\frac{1}{k_q}$, τ – lifetime

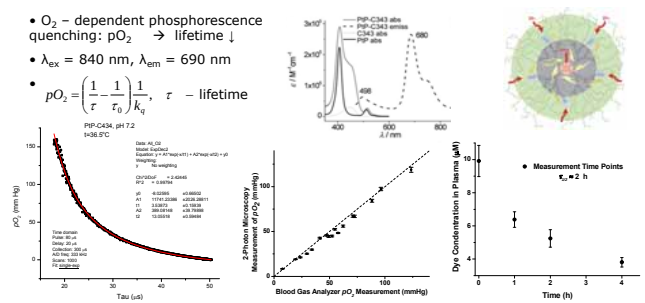

Intravascular pO_2 Measurement

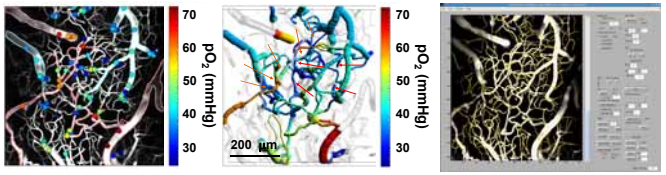

Colored dots represent point measurements of pO_2. Measurements at selected locations were typically obtained every Δz = 50 µm up to a depth of 450 µm. pO_2 points are plotted over the MIP of the vasculature stack. Pial arteries and veins are false colored for easier identification. Measurement of pO_2 values is possible in all micro vessels, including capillaries (red arrows). pO_2 can be measured in consecutive vasculature branches, from pial arterioles, down to capillaries and further to ascending venules (orange arrows).

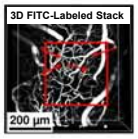

pO_2 Distribution in Cortical Tissue

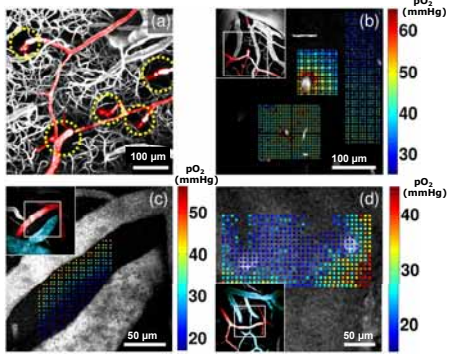

pO_2 Distribution in Diving Arterioles

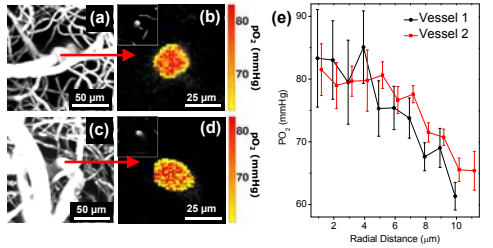

(a) 660 µm thick MIP of microvasculature with FITC-labeled blood plasma. **(b)** pO2 inside the diving arteriole at the center of (a). Insert shows FITC plane from (a) at 126 µm depth with the diving arteriole at the center. Vessel diameter 24 µm. pO2 in mmHg. **(c)** 560 µm thick MIP of vasculature. **(d)** pO2 inside the diving arteriole from (c) at 90 µm depth. Vessel diameter 21 µm. **(e)** pO2 dependence on radial distance from the center of the vessel (black line: (a) and (b); red line: (c) and (d)).

$CMRO_2$ Calculation - Krogh's Model and Tissue pO_2 Gradients Around Descending Arterioles

Capillary density around descending arterioles is reduced due to high tissue oxygenation. This enables application of simple Krogh's model of O_2 diffusion.

$$pO_2(r) = pO_{2art} + \frac{CMRO_2}{4D\alpha}\left(r^2 - R_{art}^2\right) - \frac{CMRO_2}{2D\alpha} R_t^2 \ln\left(\frac{r}{R_{art}}\right)$$

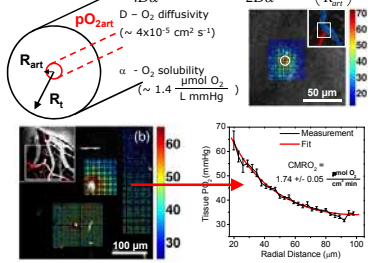

Microvascular Oxygenation as a Function of Branching Order From the Pial Vessels

Oxygenation During Baseline Conditions

Measurement of pO_2 was performed in a SI area of mice (C57BL/6, male, young adults, 23-29 g) anesthetized by 1% isoflurane in a mixture of air and oxygen. The conversion between PO2 and oxygen saturation of hemoglobin (SO2) for C57BL/6 mice was performed using the Hill equation with Hill coefficient h = 2.59 and P50 = 40.2. Microvascular graph was computed based on 3D microvascular structure obtained from the FITC-labeled blood plasma. The Floyd-Warshall algorithm was used to calculate branching orders of individual vascular segments in respect to pial vessels.

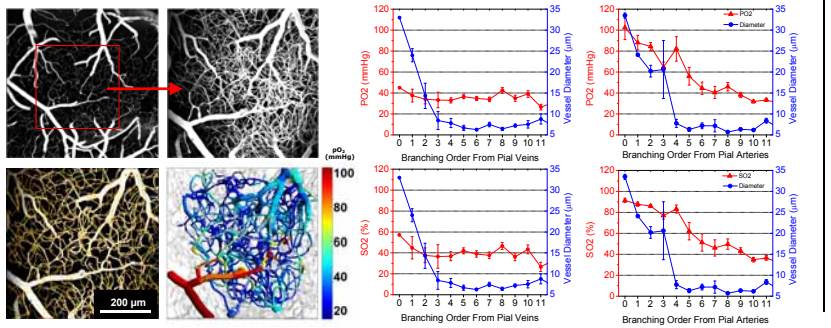

Oxygenation During Hypercapnia

Hypercapnia in tracheotomized and ventilated mice was induced by adding ~5% CO2 in a mixture of air and O2. With the help of a micro-capnograph, exact amount of CO2 in the mixture was fine tuned together with the ventilation parameters to achieve exhaled pCO2 ≈ 50 mmHg.

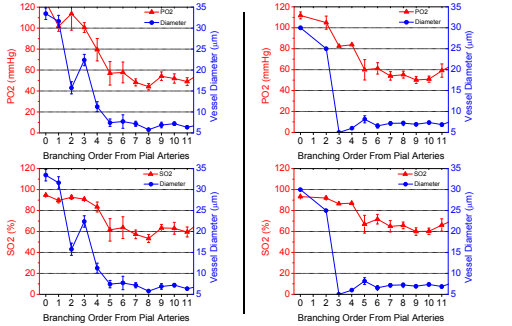

pO_2 Correction in Capillaries

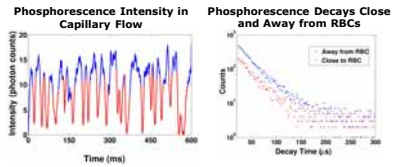

Conclusions

- Cortical tissue pO_2 maps in SI area revealed strong pO_2 gradients around both pial and descending arterioles. In contrast, we observed very heterogeneous tissue pO_2 farther from arterials without pronounced gradients around blood vessels. At some measurement locations, efflux of oxygen from tissue into ascending venules was observed.
- We obtained extensive maps of pO2 values in mice cortical microvasculature down to 450 µm depth. Based on microvascular structural images, we obtained the graphs of microvasculature and assigned to each vessel a branching order from the pial arteries and veins. Microvascular PO2 and SO2 dependence on the branching order suggests that at the baseline precapillary arterioles are responsible for significant $\Delta SO2 > 0.15$.
- The most significant increase in intravascular oxygenation due to hypercapnia-induced hyperemia was observed within the capillaries distal to the pial arterioles ($\Delta SO2 > 0.20$).

Acknowledgments

We acknowledge support from NIH grants R01NS057476, R01EB000790, P01NS055104, R01NS057198 and K99NS067050, as well as AHA grants 11SDG7600037 and 11IRG5440002.